

Exploring the Motions of Long Bubbles in Tubes

“Understanding the Bretherton Bubble Problems”

By Tristen Hohman

January 6, 2010

Abstract

A bubble of fluid with negligible viscosity is moving with some constant velocity U in a tube filled with fluid of viscosity μ at low Reynolds number. The inter-facial tension between the two fluids is denoted by γ . This bubble can be characterized in two main cases.

The first case is one in which the tube is a horizontal capillary tube of radius r such that the gravitational effect on the motion can be neglected. The bubble has a thin fluid film denoted h_∞ between it and the wall of the tube that is given by

$$\frac{h_\infty}{r} = .643 \left(\frac{3\mu U}{\gamma} \right)^{2/3} .$$

The velocity of the bubble U exceeds the average velocity of the fluid V by an amount UW where W is given by

$$W \simeq 1.29 (3\mu U / \gamma)^{2/3}$$

and W is uniquely determined by the characteristics of the leading meniscus. Finally the pressure drop across the bubble is given by

$$P \simeq 4.52 (3\mu U / \gamma)^{2/3} \gamma / r .$$

These relations are applicable only in the regime where the capillary number ($\mu U / \gamma$) is much less than unity.

The second case explored is one in which the bubble is in a vertical, closed end, fluid filled tube of larger diameter where the gravitational effects on the bubble motion are now important and appear with the inclusion of a buoyancy force on the bubble. It is found from statics of the bubble that there exists a critical value of the bond number such that when

$$\rho g r^2/\gamma < 0.842 \quad ,$$

where ρ is the density difference across the bubble, the bubble will not rise in the tube. The range of bond number considered by Bretherton (1961) is

$$0.842 < \rho g r^2/\gamma < 1.04 \quad ,$$

where the relation

$$\rho g r^2/\gamma - 0.842 \simeq 1.10(h_\infty/r)^{2/3} + 1.85(h_\infty/r) \simeq 1.25(\mu U/\gamma)^{2/9} + 2.24(\mu U/\gamma)^{1/3}$$

is applicable.

1. Introduction

In many physical experiments, fluid flow rates are measured by passing the fluid through a capillary tube of radius r containing an air bubble of length several times that of the tube diameter. By observing the motion of the bubble, the flow rate of the fluid can be found. This idea is employed in many experiments such as one by Prothero and Burton (1962) to model red blood cell movement in capillaries and in another by Slavik and Jarvis (1974) through the use of potometers to measure the rate of water uptake by a leafy plant. However, this bubble velocity U was found by Fairbrother and Stubbs (1935) to be greater than the average fluid velocity V by the quantity UW . The only forces on the bubble are those due to viscous stresses, surface tension stresses, the stresses resulting from a uniform pressure inside the bubble, from inertia, and from gravity. If the radius of the tube is small enough then the effect of gravity will be negligible and there will exist a uniform thin film of fluid along the walls of the tube between the front and rear menisci. This thin film has a thickness h_∞ and occurs over a section of the bubble that has a length much larger than the tube diameter. In this section the fluid has a uniform pressure and experiences no tangential stress at the interface meaning the fluid in the film is at rest. This allows us to characterize the meaning of W through the use of a mass balance for a control volume moving with the bubble at speed U . This approach says that the volume flux through the thin

film equals the volume flux in the open tube and is given by the relation

$$-(0-U)A_{film}+(V-U)A_{tube}=0$$

where A_{film} and A_{tube} are the cross-sectional area of the film and tube respectively. Notice that although the fluid is at rest in the thin film, the velocity of the fluid in the thin film relative to the moving control volume is $-U$. Simplifying this relation we get

$$U(A_{tube}-A_{film})=VA_{tube} \quad \text{where} \quad A_{tube}-A_{film}=A_{bubble}=\pi(r-h_{\infty})^2 \quad \text{so} \quad U\pi(r-h_{\infty})^2=V\pi r^2 \quad .(1)$$

The average velocity of the fluid in the tube is related to the speed of the bubble by

$$V=U-UW$$

so the ratio of the average fluid speed to the speed of the bubble is given by

$$\frac{V}{U}=\frac{U(1-W)}{U}=1-W=\left(1-\frac{h_{\infty}}{r}\right)^2 \quad (2)$$

so the quantity W , and therefore the relationship between the fluid flow rate and bubble speed, is found solely by calculating the thickness of the thin film h_{∞} .

The first case studied by Bretherton is the case of a long bubble with steady velocity U moving in a capillary tube of radius r . The fluid is assumed to wet the walls of the tube and the inter-facial tension of the bubble is assumed to be well defined and constant implying that the tangential viscous stresses at the interface vanish. We will assume that the Reynolds number based on the tube radius is small and that the gravitational forces can be ignored when compared to the surface tension forces or

$$\rho r U / \mu \ll 1 \quad \text{and} \quad \text{Bond Number} = \rho g r^2 / \gamma \ll 1$$

respectively. These assumptions will be discussed further in §2. Now the only forces that act on the bubble are viscous forces and surface tension forces. This means that a dimensional argument can be made to state that the value of h_{∞}/r , and therefore W , is solely determined by a function of the dimensionless group $\mu U/\gamma$, also known as the capillary number.

The second case studied is the one in which there is a bubble in a fluid filled vertical tube of radius r with a closed end. Again the fluid is assumed to completely wet the walls and the Reynolds

number based on the radius of the tube is small but the effect of gravity cannot be neglected. A dimensional argument for the speed of rise U of the bubble can be made using two dimensionless groups, the capillary number and the bond number, given by

$$\mu U l \gamma = f(\rho g r^2 l \gamma) \quad . \quad (3)$$

In both of these cases we can say that for sufficiently small capillary number the viscous stresses are only important in the region of the bubble very close to the wall where a “lubrication approximation” becomes valid while in the center of the tube a static meniscus profile is a good description of the bubble shape. In the intermediate region these two regimes are “stitched together” using asymptotic matching to give an estimate of the entire bubble profile.

2. Bubble in a Capillary Tube

(i) The first case examined is the one in which a bubble of fluid with negligible viscosity is placed in a horizontal capillary tube filled with a fluid of viscosity μ . This fluid has an average velocity denoted by V , and the bubble, which has a length much greater than the tube radius, has a velocity denoted by U . Two assumptions about the forces acting on the bubble can be made for this case. The first is that the inertial forces are small enough so that the profile of the static menisci is unchanged. This means that the ratio of inertial to viscous forces is only important in the region near the wall and that the relevant Reynolds number is the one involving the length scale of the thin film h_∞ . This is also paired with a ratio of the thin film thickness to the length scale of the dynamic region given by

$$L \propto r (\mu U l \gamma)^{1/3} \quad .$$

The Reynolds number is given by

$$\frac{\rho U h_\infty}{\mu} \frac{h_\infty}{L}$$

where it will later be seen that

$$h_\infty \propto r (\mu U l \gamma)^{2/3}$$

therefore the necessary condition to neglect the inertial forces on the bubble is not $\rho U r / \mu \ll 1$ but is actually

$$\rho r U^2 / \gamma \ll 1 \quad . \quad (4)$$

The second assumption that can be made is that the tube diameter is sufficiently small, then the timescale for the fluid in the thin film to drain to the lowest generator of the tube is much longer than the timescale for the bubble to move one tube diameter. This will be true if the ratio of gravitational forces to viscous forces is small, i.e. if

$$\rho g h_\infty^2 / \mu U \ll 1$$

or, using the form of the thin film thickness,

$$(\rho g r^2 / \gamma)(\mu U / \gamma)^{1/3} \ll 1 \quad . \quad (5)$$

This relation differs from the one stated in §1 by its multiplication with the capillary number to the one third power. With these two assumptions, only the viscous forces and surface tension forces play a role in the bubble motion.

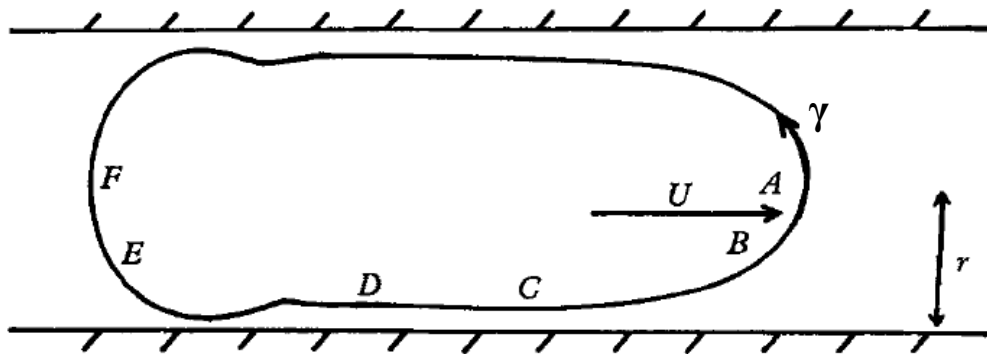


FIGURE 1. Section of a bubble in a horizontal tube.

(ii) For a static bubble in the tube, the viscous stresses vanish and the menisci profiles will be determined solely by the surface tension of the interface. Assuming the bubble is axisymmetric, the menisci will have constant mean curvatures. The only axisymmetric shape that does not have a singularity on the axis and also satisfies the condition of zero contact angle at the wall is a hemisphere. When the capillary number is sufficiently small and non-zero, the bubble profile can be split into sections as seen in figure 1. In regions AB and EF, the shape of the profile will still resemble a

spherical section, as in the static bubble case, and therefore the curvature κ_1 is $2/r$. There will also be a region CD where there is a thin film with thickness h_∞ where it is assumed that $h_\infty/r \ll 1$ and therefore the curvature κ_1 is $1/(r-h_\infty)$ or approximately $1/r$. Finally there are two transition regions, BC and DE, where the profile transitions from the thin film region CD to the static menisci in regions AB and EF.

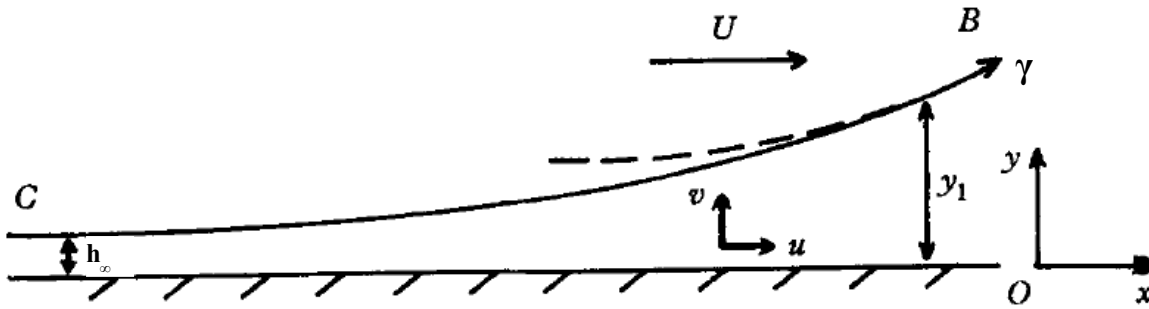


FIGURE 2. The transition region.

(iii) The transition regions BC and DE are now considered in greater detail using the notation in figure 2. For a sufficiently small capillary number the interface in this region, $y = y_1$, can be considered to be nearly parallel to the wall, therefore, the “lubrication approximation” used by Landau and Levich (1942) is an appropriate description of the flow in this transition region. Using this method the bubble profile can be considered in the strictly planar case without any loss of generality. Also, the slope of the interface in this region is very small, i.e. $dy_1/dx \ll 1$, and the pressure p_1 within the film is strictly a function of x . The fluid in the tube has a velocity component in the x -direction only, u , and the x -derivatives of the velocity are negligible compared to the corresponding y -derivatives. From a force balance on the interface, the tangential and normal stress conditions can be derived. The tangential stress condition reduces to

$$u_y = 0 \quad \text{when} \quad y = y_1 \quad (6)$$

because the tangential stress at the interface has to be zero by definition. The normal stress condition at the interface,

$$p_1 + \gamma \kappa_1 = -2\mu \{1 + (dy_1/dx)^2\}^{1/2} u_x, \quad \text{with} \quad \kappa_1 = \frac{d^2 y_1}{dx^2} + \frac{1}{r}$$

where κ_1 is the total curvature using the assumption that the in-plane curvature is slowly changing. The normal stress condition can then be reduced to

$$p_1 = -\gamma \left(\frac{d^2 y_1}{dx^2} + \frac{1}{r} \right) . \quad (7)$$

These conditions along with, steady flow, small Reynolds number, and negligible gravity, result in the following reduced Navier-Stokes equations,

$$\underline{0} = -\underline{\nabla} p + \mu \nabla^2 \underline{u} \quad \text{or} \quad u_{yy} = \frac{1}{\mu} \frac{dp_1}{dx} , \quad (8)$$

subject to the boundary condition

$$u = 0 \quad \text{at} \quad y = 0 . \quad (9)$$

Repeated integration of (7) and the use of the boundary conditions (6), (7), and (9) yields the functional form of the fluid velocity profile in the transition region given by

$$u(x, y) = \frac{1}{2\mu} \frac{dp_1}{dx} (y^2 - 2y_1 y) . \quad (10)$$

The volume flux of the fluid through the thin film at any value of x is given by the equation

$$\tilde{V} = 2\pi \int_{r-y_1}^r (u R) dR \quad \text{or changing coordinates} \quad \tilde{V} = 2\pi \int_0^{y_1} u r \left(1 - \frac{y}{r} \right) dy ,$$

but noting that the ratio y/r is much less than unity and substituting (10) in for the function u gives an approximate value for the volume flux given by

$$\tilde{V} = 2\pi \int_0^{y_1} u r dy = -2\pi r \frac{y_1^3}{3\mu} \frac{dp_1}{dx} . \quad (11)$$

Using continuity, the flux of the fluid past the bubble must equal

$$\tilde{V} = 2\pi r U (y_1 - c) \quad (12)$$

where c is a constant needed to account for the greater velocity of the bubble with respect to the fluid.

This condition can be combined with (11) and the pressure boundary condition (7) to find an ODE for the shape of the interface given by

$$\frac{d^3 y_1}{dx^3} = \frac{3\mu U}{\gamma} \frac{y_1 - c}{y_1^3}, \quad (13)$$

but when $y_1 = h_\infty$, $d^3 y_1 / dx^3 = 0$ so therefore $c = h_\infty$. This ODE describes the profile of the bubble in the region BCDE and can be non-dimensionalized using the substitutions

$$y_1 = h_\infty \eta \quad \text{and} \quad x = h_\infty (3\mu U / \gamma)^{-1/3} \xi. \quad (14)$$

Then the ODE in (13) becomes

$$\frac{d^3 \eta}{d\xi^3} = \frac{\eta - 1}{\eta^3}. \quad (15)$$

(iv) To combine the static regions with the transition regions, one must realize that given a solution of (15) and assuming that the capillary number is sufficiently small, there exists a region in which

$$\eta = y_1 / h_\infty \gg 1 \quad \text{and} \quad y_1 / r = h_\infty \eta / r \ll 1 \quad \text{but} \quad \frac{dy_1}{dx} = \left(\frac{3\mu U}{\gamma} \right)^{1/3} \frac{d\eta}{d\xi} \ll 1,$$

such that the ODE derived in (15) still applies. Therefore, (15) can be reduced to $d^3 \eta / d\xi^3 \approx 0$ in this region and can be integrated three times to give the expression

$$\eta \approx \frac{1}{2} P \xi^2 + Q \xi + R \quad (16)$$

with arbitrary constants P, Q, and R. Equations (14) can be used to find the profile of the bubble in this region given by

$$y_1 \approx \frac{1}{2} P \left(\frac{3\mu U}{\gamma} \right)^{2/3} \frac{x^2}{h_\infty} + Q \left(\frac{3\mu U}{\gamma} \right)^{1/3} x + R h_\infty, \quad (17)$$

which yields the following equation for the total curvature in this region

$$\kappa_1 \approx \frac{d^2 y_1}{dx^2} + \frac{1}{r} \approx \left(\frac{3\mu U}{\gamma} \right)^{2/3} \frac{P}{h_\infty} + \frac{1}{r}. \quad (18)$$

This is a constant value for the curvature and shows that the shape of the bubble is determined solely by surface tension forces. Therefore this constant curvature can be extended past B and E into the regions AB and EF where the curvature is approximately the curvature of a sphere, $2/r$. Although the

analysis to find (18) does not apply in these regions, the viscous stresses must still be negligible compared to the surface tension stresses. Applying this idea to (18) shows that an additional relationship can be defined

$$\frac{h_{\infty}}{r} = P \left(\frac{3\mu U}{\gamma} \right)^{2/3} . \quad (19)$$

In the region CD, $y_1 \simeq h_{\infty}$ and therefore $\eta \simeq 1$ and (15) reduces through a Taylor expansion to $d^3\eta/d\xi^3 \simeq \eta - 1$ which has the general solution

$$\eta = 1 + \alpha e^{\xi} + \beta e^{-\xi/2} \cos(\sqrt{3}\xi/2) + \lambda e^{-\xi/2} \sin(\sqrt{3}\xi/2) . \quad (20)$$

This equation can be split into two equations by considering the way it behaves near either end of region CD. If $(l/h_{\infty})(3\mu U/\gamma)^{1/3} \gg 1$ where l is the length of region CD, then (20) will be dominated by the first two terms near C,

$$\eta - 1 \simeq \alpha e^{\xi} , \quad (21)$$

and will be dominated by the first, third, and fourth terms near D,

$$\eta - 1 \simeq \beta e^{-\xi/2} \cos(\sqrt{3}\xi/2) + \lambda e^{-\xi/2} \sin(\sqrt{3}\xi/2) . \quad (22)$$

This indicates that the front and rear menisci are treated separately from each other and that the transition regions BC and DE are also fundamentally different.

(v) First treating the front meniscus, we can eliminate the constant α by suitably choosing the origin of ξ such that $\alpha=1$. This shows that there is a unique solution of (15) near C and through numerical integration in the direction of increasing ξ looking for a constant curvature we can find unique values of P, Q, and R. However, you can also choose the origin such that Q vanishes and this will merely have the effect of shifting the position of the bubble in the tube and will not change its shape. Performing this integration gives the results $P = 0.643$, $Q = 0$, and $R = 2.79$, which can be substituted into (19) to yield

$$h_{\infty}/r = 0.643(3\mu U/\gamma)^{2/3} . \quad (23)$$

This is then substituted into (17) to give the profile of the bubble near B,

$$y_1 = \frac{1}{2}(x^2/r) + 1.79(3\mu U/\gamma)^{2/3}r \quad . \quad (24)$$

This equation is an accurate extension of the hemispherical front meniscus in the region BC and is shown as the dashed curve in figure 2. This virtual hemisphere has a tangent parallel to the wall at $x=0$ at a distance from the center of the tube,

$$r - y_1(0) = r\{1 - 1.79(3\mu U/\gamma)^{2/3}\} \quad . \quad (25)$$

Therefore the corrected curvature in region AB is given by

$$\kappa_1 = (2/r)\{1 - 1.79(3\mu U/\gamma)^{2/3}\}^{-1}$$

or by Taylor expansion

$$\kappa_1 = (2/r)\{1 + 1.79(3\mu U/\gamma)^{2/3}\} \quad . \quad (26)$$

This small difference from $2/r$ does not invalidate the result in (19) but (26) allows us to estimate the pressure drop across the front meniscus that arises from the surface tension stresses

$$(2\gamma/r)\{1 + 1.79(3\mu U/\gamma)^{2/3}\}$$

and the dynamic pressure drop across the front meniscus is

$$3.58(3\mu U/\gamma)^{2/3}(\gamma/r) \quad . \quad (27)$$

(vi) At the rear meniscus we now use (22) which has two constants β and λ . One of these constants can be made unity by the same method as in (v) but the other will remain. You can then find that using numerical integration any value of $P \geq 0$ is possible by varying the remaining constant and therefore there is no unique solution. However, for a given ratio of h_x/r determined by the front meniscus, there exists a unique solution of (15). This ratio is given in (23) which can be used to determine the dynamic pressure drop across the rear meniscus as

$$-0.930(3\mu U/\gamma)^{2/3}(\gamma/r) \quad (28)$$

which, when combined with the dynamic pressure drop across the front meniscus, gives the total dynamic pressure drop as

$$4.52(3\mu U/\gamma)^{2/3}(\gamma/r) \quad . \quad (29)$$

(vii) Finally we can calculate the value of the velocity correction factor W. Solving for W in (2) yields

$$W = -(h_{\infty}/r)^2 + (2h_{\infty}/r) \quad ,$$

but since $h_{\infty}/r \ll 1$ this can be reduced to

$$W = 2h_{\infty}/r \quad . \quad (30)$$

Substituting (23) into (30) yields

$$W = 1.29(3\mu U/\gamma)^{2/3} \quad . \quad (31)$$

3. Bubble in a Vertical Tube

(i) In the second case considered by Bretherton, the bubble is in a vertical fluid filled tube of radius r that is sealed at one end. Because of the vertical orientation it is clear that gravity will now play a significant role in the bubble motion through a buoyant force acting on the bubble. Inertial forces can be neglected as in §2 but the relevant Reynolds number is considered differently. We still start with the initial form of the Reynolds number used in the horizontal capillary tube case

$$\frac{\rho U h_{\infty}}{\mu} \frac{h_{\infty}}{L} \quad ,$$

only now the length scale of the variations downstream are given by

$$L \propto h_{\infty} (\rho g h_{\infty}^2 / \gamma)^{-1/3} \quad .$$

Therefore after applying a continuity equation that will be shown later, the necessary condition required to neglect the effects of inertial forces is

$$\frac{\rho U r}{\mu} \left(\frac{\rho g h_{\infty}^2}{\gamma} \right)^{1/3} \ll 1 \quad . \quad (32)$$

Assuming that the steady rise of the bubble U is slow enough such that the capillary number is small, the effect of the viscous forces on the bubble will be small in the center of the tube and will only have effect near the wall. This allows us the use of a “lubrication approximation” in the same way as it was

used in the horizontal capillary tube analysis.

(ii) An interesting phenomena that was observed by Bretherton was that for a bond number lower than a critical value, the bubble remained motionless in the tube and the effects of the buoyant force appeared to be offset. Since the bubble was at rest the viscous forces vanish and it would seem that there were no forces available to offset the effects of gravity. The only explanation that one could come to is that the hydrostatic forces deform the profile of the bubble in such a way that it effectively plugs the tube and a “frictional” force from the walls of the tube keep the bubble stationary. With this idea for motivation one can analyze the shape of the bubble under static conditions using a tangent angle arc length estimation. Using this estimation of the shape with the origin placed at the front of the bubble with positive z pointing down and the angle ϕ measured from the vertical such that ϕ decreases as z increases, a dimensionless equation for the shape of the interface is given by

$$\frac{d\phi}{dS} = \frac{-\rho g r^2}{\gamma} Z + \frac{\cos(\phi)}{H} + c = -BZ + \frac{\cos(\phi)}{H} + c, \quad \frac{dH}{dS} = \sin(\phi), \quad \text{and} \quad \frac{dZ}{dS} = \cos(\phi), \quad (33)$$

where r is the radius of the tube, B is the bond number, and c is a constant. Using numerical integration for different values of the bond number shows that the critical value of the bond number under which the bubble will not rise is

$$\rho g r^2 / \gamma < 0.842. \quad (34)$$

(iii) The bubble has a profile, shown in figure 3, that can be divided similarly to the way it was in figure 1. There are regions at both ends of the bubble that appear to have menisci whose shapes are solely determined as if they are static. Numerical analysis done by Bashforth and Adams (1883) on the shapes of pendant and sessile drops, was extended by Fordham (1948) and Bretherton himself to describe the possible shapes of these static regions, AB and EF. These possible shapes, seen in figure 4, were split into two cases for the top menisci and only one case for the bottom menisci. Both of the possible cases for the top meniscus have an inflexion point I at which the radius is denoted by r_I . This radius of inflexion defines the differences between the two cases. Figure 4(a) displays the case when

$\rho g r_l^2 / \gamma > 0.842$ and the tangent plane to the curve is never vertical while figure 4(b) displays the case when $\rho g r_l^2 / \gamma < 0.842$ and the tangent plane is vertical at a point T. Bretherton states that the most important region of interest in this problem is the region

$$0.842 < \rho g r_l^2 / \gamma < 1.04 \quad . \quad (35)$$

Using a numerical integration method similar to that used in part (ii), the angle formed by the tangent plane to the profile and the vertical can be found to be

$$\phi = 0.49 \{ (\rho g r_l^2 / \gamma) - 0.842 \} \quad . \quad (36)$$

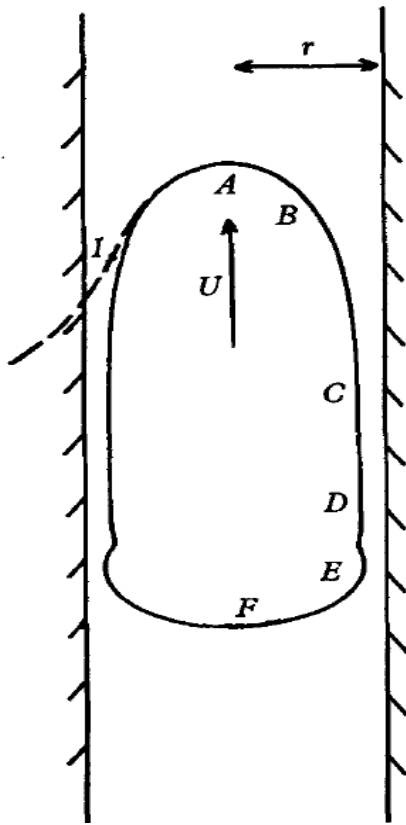


FIGURE 3. Section of a bubble in a vertical tube.

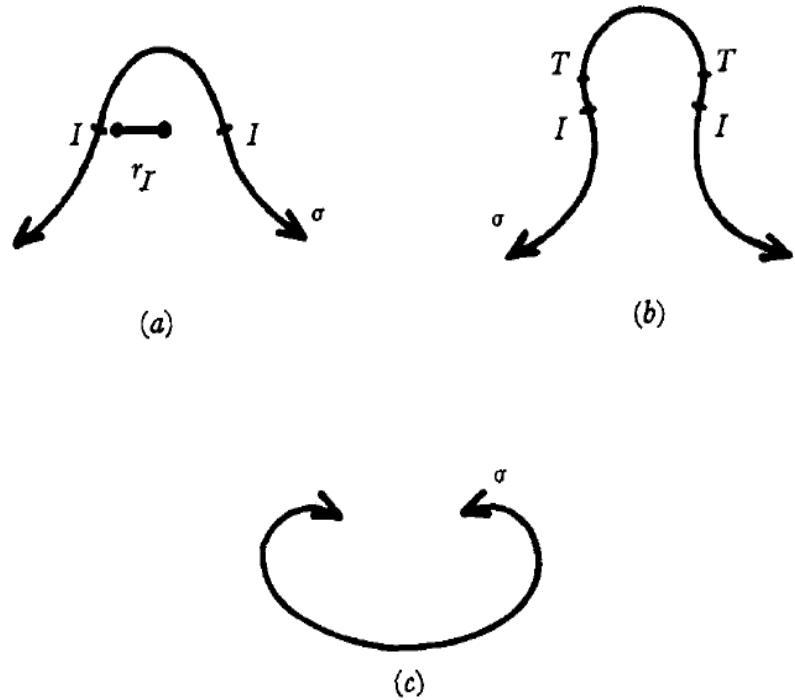


FIGURE 4. Equilibrium profiles under surface tension and gravity forces. (a) Top meniscus $\rho g r_l^2 / \gamma > 0.842$; (b) top meniscus $\rho g r_l^2 / \gamma < 0.842$; (c) bottom meniscus.

(iv) The transition and uniform regions, BCDE, can now be analyzed similar to the manner in which the horizontal capillary tube problem was analyzed with the exception of an additional term from gravity. Assuming that the rise of the bubble is sufficiently slow, the lubrication approximation can again be used. Using the notation for this region shown in figure 5, the tangential and normal stress conditions in this region are the same as those in (6) and (7) respectively. With these boundary

conditions along with the assumptions in (I), namely the relevant Reynolds number is low, the capillary number is small, and the rise of the bubble is steady, the Navier-Stokes equations can be written as

$$\Omega = -\nabla p + \mu \nabla^2 u + f$$

where f is the additional pressure force due to gravity acting in the negative x -direction. This equation can be solved for the x -component which yields a differential equation for the velocity in the fluid given by

$$u_{yy} = \frac{1}{\mu} \left(\frac{dp_1}{dx} + \rho g \right) \quad (37)$$

This equation can be integrated twice subject to (6) and a no-slip condition at the wall resulting in the equation for the fluid in the gap

$$u(x, y) = \left(\frac{1}{2} \frac{y^2}{\mu} - \frac{y_1 y}{\mu} \right) \left(\frac{dp_1}{dx} + \rho g \right) \quad (38)$$

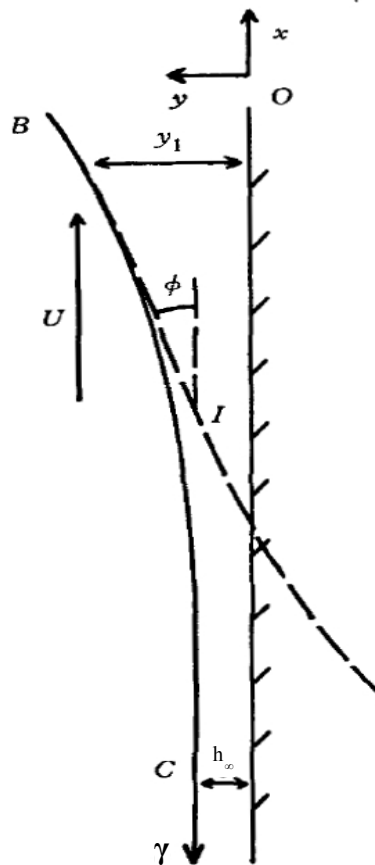


FIGURE 5. The top transition region.

The volume flux past the bubble is given by

$$\tilde{V} = 2\pi r \int_0^{y_1} u dy + V_f \quad (39)$$

where V_f is the volume flux through the thin film because of gravity which has the form

$$V_f = 2\pi r \frac{\rho g h_\infty^3}{3\mu} .$$

By continuity, the volume flux past the bubble must also equal the volume of fluid passing by the rising bubble or

$$\tilde{V} = 2\pi r U (y_1 - c) . \quad (40)$$

Combining these equations with the second boundary condition (7) gives the result

$$\frac{d^3 y_1}{dx^3} - \frac{\rho g}{\gamma} = \frac{3\mu U}{\gamma} \frac{1}{y_1^3} \left(y_1 - h_\infty - \frac{\rho g h_\infty^3}{3\mu U} \right) \quad (41)$$

because when $y_1 = h_\infty$, $d^3 y_1 / dx^3 = 0$ so $c = h_\infty$. However, there is an additional continuity requirement which states that the volume flux through the uniform region must equal the fluid displaced by the top of the rising bubble or that

$$2\pi r \frac{\rho g h_\infty^3}{3\mu} = V_f = U \pi (r - h_\infty)^2 \quad \text{or} \quad \frac{\rho g h_\infty^2}{3\mu} = U \left(\frac{r}{2h_\infty} - 1 + \frac{h_\infty}{r} \right) .$$

For sufficiently small capillary number, $h_\infty / r \ll 1$ and these equations can be reduced to

$$\frac{\rho g h_\infty^2}{3\mu U} \simeq \frac{r}{2h_\infty} . \quad (42)$$

With this condition one can easily see that the last term on the right hand side of equation (41) is of much greater magnitude than the first two terms. This will hold as long as the capillary number is sufficiently small, however, this is already a precondition for (42). With this simplification, (41) becomes

$$\frac{d^3 y_1}{dx^3} = \frac{\rho g}{\gamma} \left(1 - \frac{h_\infty^3}{y_1^3} \right) \quad (43)$$

which can be non-dimensionalized by

$$y_1 = h_\infty \eta \quad \text{and} \quad x = h_\infty (\rho g h_\infty^2 / \gamma)^{-1/3} \xi \quad (44)$$

to give the general differential equation

$$\frac{d^3 \eta}{d \xi^3} = \frac{\eta^3 - 1}{\eta^3} \quad (45)$$

(v) To combine the static regions with the transition region, we will follow the same procedure as set forth in (iv) of §2. Therefore for a sufficiently small bond number as well as a sufficiently small capillary number, there will exist a region in which

$$\eta = y_1 / h_\infty \gg 1, \quad y_1 / r = h_\infty \eta / r \ll 1 \quad \text{and yet} \quad \frac{dy_1}{dx} = \left(\frac{\rho g h_\infty}{\gamma} \right)^{1/3} \frac{d\eta}{d\xi} \quad (46)$$

such that the ODE derived in (43) still applies. Using (46), equation (45) becomes $d^3 \eta / d \xi^3 \simeq 1$ and can be integrated three times to give

$$\eta \simeq \frac{1}{6} \xi^3 + \frac{1}{2} P \xi^2 + Q \xi + R \quad (47)$$

where P, Q, and R are constants. If we resubstitute the equations in (44) into (47) we find

$$y_1 \simeq \frac{1}{6} \frac{\rho g}{\gamma} x^3 + \frac{P}{2} \frac{(\rho g h_\infty^2 / \gamma)^{2/3}}{h_\infty} x^2 + Q (\rho g h_\infty^2 / \gamma)^{1/3} x + R h_\infty \quad (48)$$

Using the boundary condition from (7), in this region

$$\frac{d \kappa_1}{dx} \simeq \frac{d^3 y_1}{dx^3} \simeq \frac{\rho g}{\gamma}$$

which represents a region of constant first derivative of curvature or a balance between surface tension forces and gravity. This is exactly the case in regions AB and EF and therefore the profiles in these regions must be defined by (47). In region CD, $y_1 \simeq h_\infty$ or $\eta \simeq 1$ and therefore by a Taylor expansion (45) becomes $d^3 \eta / d \xi^3 \simeq 3(\eta - 1)$ which has the general solution

$$\eta = 1 + \alpha e^{3^{1/3} \xi} + \beta e^{-3^{1/3} \xi / 2} \cos(3^{5/6} \xi / 2) + \lambda e^{-3^{1/3} \xi / 2} \sin(3^{5/6} \xi / 2) \quad (49)$$

Near C, the last two terms become small and

$$\eta - 1 = \alpha e^{3^{1/3} \xi} \quad (50)$$

while, near D the second term becomes small and

$$\eta - 1 = \beta e^{-3^{1/3}\xi/2} \cos(3^{5/6}\xi/2) + \lambda e^{-3^{1/3}\xi/2} \sin(3^{5/6}\xi/2) \quad . \quad (51)$$

It can then be shown that through a suitable change of origin that (50) is a unique solution of (45) and therefore the top meniscus has a unique profile, while the bottom meniscus is made of an infinite family of profiles. However using the same approach as before a the bottom meniscus can be made unique through the inclusion of the ratio h_∞/r found by the front meniscus. It can be shown that the top meniscus cannot be of type 4(b) because there is no point where $d\eta/d\xi=1$ and therefore there is no point where the tangent plane is vertical. Numerical integration of (45) for the top meniscus subject to the constraint of a constant first derivative of curvature and with the origin chosen such that $P=0$, yields the constants

$$P=0, \quad Q=0.572, \quad R=1.10 \quad .$$

Using these constants in (48) at the point of inflexion I,

$$y_1 = 1.10h_\infty, \quad dy_1/dx = 0.572(\rho g h_\infty^2/\gamma)^{1/3}, \quad r_I = r - y_1 \quad (52)$$

which can be substituted into (36) along with the relation $\tan(\phi) = dy_1/dx$ and a small angle approximation to give

$$\phi = 0.49 \left\{ \frac{\rho g h_\infty^2}{\gamma} \left(1 - 1.10 \frac{h_\infty}{r} \right)^2 - 0.842 \right\} = 0.572 \left(\frac{\rho g h_\infty^2}{\gamma} \right)^{1/3} \quad . \quad (53)$$

This can be further simplified with a couple of approximations. First the parentheses on the left hand side can be expanded using a Taylor series. Next, since the bond number is only slightly greater than 0.842, anywhere the bond number appears on the right hand side it will be replaced with 0.842. Finally the continuity condition from (42) can be used to relate h_∞/r to the capillary number. Using these approximations (53) becomes

$$\begin{aligned} \frac{\rho g r^2}{\gamma} - 0.842 &= 1.10 \left(\frac{h_\infty}{r} \right)^{2/3} + 1.85 \frac{h_\infty}{r} \\ &= 1.25 \left(\frac{\mu U}{\gamma} \right)^{2/9} + 2.24 \left(\frac{\mu U}{\gamma} \right)^{1/3} \quad . \quad (54) \end{aligned}$$

This equation then provides the relationships between the ratio of the thin film thickness to the radius of the tube, the bond number, and the capillary number and justifies the result provided by dimensional analysis.

4. Experimental Results

(I) In the horizontal capillary tube case there were a few different experiments performed before Bretherton that all gave conflicting results. Fairbrother and Stubbs (1935) used a 2mm diameter Veridia glass tube and measured the volume of liquid ejected when the bubble traveled a known distance. They would then compare these two volumes to find the proportion of fluid left on the walls, W . They found this quantity to be

$$W = 1.0(\mu U/\gamma)^{1/2} \quad \text{for } \mu U/\gamma < 0.015 \quad .$$

Not only was this experiment limited in the ranges of capillary number it explored, but it was also suffering from the fact that the volume of fluid was measured in two different ways and any error in the measurements of these small volumes would effect the value of W greatly. Marchessault and Mason (1960) later tried to measure the thickness of the film left behind on the walls of the tube by measuring the resistance of the tube containing a bubble of known length. Using this method they suggested that the correction factor W be

$$W = (\mu/\gamma)^{1/2}(-0.10 + 1.78/U^{1/2}) \quad \text{for } 7 \times 10^{-6} < \mu U/\gamma < 2 \times 10^{-4} \quad .$$

Bretherton (1960) was unhappy with any of these results as they differed greatly from his theoretical calculations. He then decided to perform his own experiment to validate the calculations he had made. His setup, shown in figure 6, was a horizontal piece of highly cleaned and dried Veridia glass tube of 1mm in diameter. A fluid column LM was drawn along at a rate of 100 cm/s by a constant head of Shell Diala oil maintained by three taps, F1, F2, F3. The fluid column was photographed near points H and K where the length of the column was measured and the distance traveled was determined. The

proportion W was then determined by the change in length of the column, divided by the distance traveled between photographs. This gave very accurate results at higher capillary numbers, but the data at lower capillary numbers showed some discrepancies that Bretherton was unable to account for. His data as well as the suggested relations from the other two experiments are plotted in figure 7.

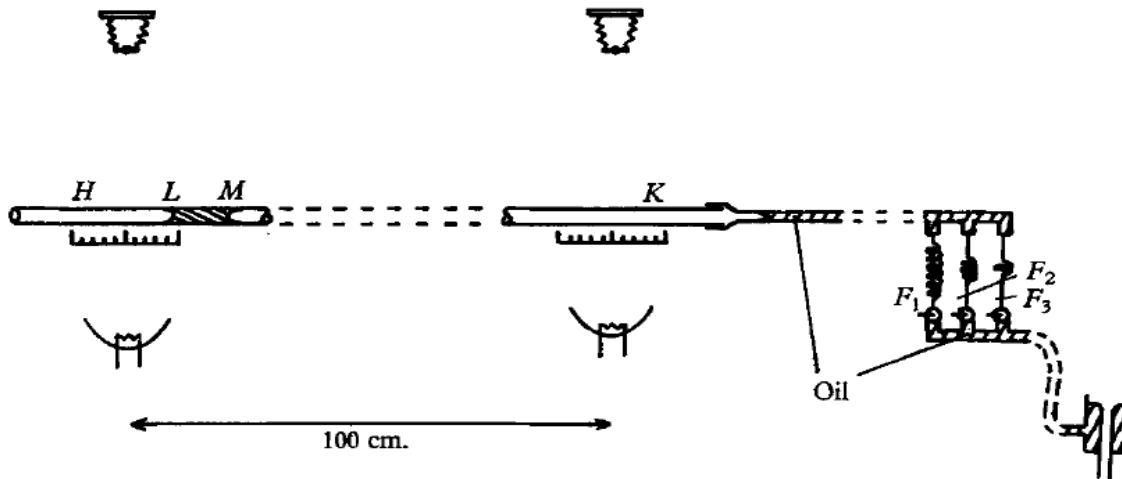


FIGURE 6. Bretherton's Experimental Apparatus.

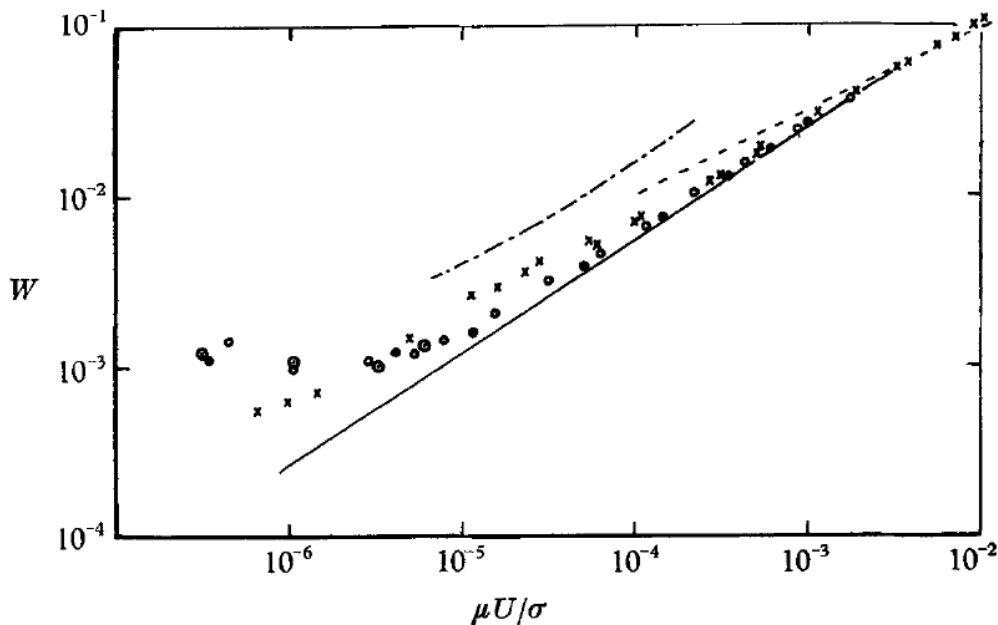


FIGURE 7. — Theory; —·— Marchessault & Mason; ---- Fairbrother & Stubbs; × aniline, O benzene (horizontal tube), ⊙ benzene (with evaporation precautions), ● benzene (vertical tube).

The current theory set forth to explain the discrepancies from the theoretical calculations observed by Bretherton is from Ratulowski and Chang (1990) and suggests that surfactants resulting from

impurities in the experiment result in an additional Marangoni effect that alters the value of W .

(ii) In the vertical tube case Bretherton gives much less experimental justification because to perform such an experiment and to have the bubble rise steadily requires a tube diameter that is very near the critical value for any given fluid. However, he found that a 0.5cm diameter tube using water at 20 °C gives a bond number equal to 0.842. He immersed this rod in a bath in which he could control the temperature of the water. For 15 °C the bond number was 0.834 and the bubble was usually stationary. For 40 °C the bubble rose steadily at a rate of a few centimeters per hour. This justified his prediction of 0.842 being the critical value of the bond number, below which the bubble would not rise. The steady rise of the bubble also qualitatively verified equation (54).

5. Conclusion

The theories presented in this paper reflect the work of Bretherton on predicting the profile of a bubble in a capillary tube and the rate of rise of a bubble in a vertical tube, and are subject to several key assumptions. The liquid interface is assumed to have a well defined tension and be free of any tangential stresses. The fluid is also assumed to perfectly wet the walls of the tube. If the speed of the bubble is sufficiently slow then inertial effects can be neglected and provided the thin film left on the wall by the bubble is sufficiently thin, then the viscous forces acting on the bubble can be described using the lubrication approximation and can be confined to a region near the wall. For the rest of the bubble, the menisci can be described using a static equilibrium approach. These two regions are then matched together using numerical integration on a differential equation describing the shape subject to some condition on the curvature upstream. This approach shows that the thickness of the thin film is determined solely by the shape of the front meniscus and that the shape of the rear meniscus is determined by a single solution that matches smoothly to the thin film of fluid left by the passing front meniscus. In the horizontal capillary tube it is found that the bubble moves slightly faster than the average velocity of the fluid in which it travels, and that this correction is given by $1.29(3\mu U/\gamma)^{2/3}$.

The main pressure drop across the bubble at the slowest speeds is the dynamic pressure drop that results from the slight differences in static curvatures of the front and rear menisci and is $4.52(\gamma/r)(3\mu U/\gamma)^{2/3}$. All of these results are only valid for capillary numbers smaller than 5×10^{-3} .

A bubble in a vertical sealed tube will not rise freely if the bond number is below a critical value of 0.842. This is the result of the bubble making zero angle of contact with the wall of the tube and therefore restricting its motion. The bubble will rise steadily at radii up to 12% larger than those of the critical value and the rate of rise is given by the equation

$$(\rho g r^2/\gamma) - 0.842 = 1.25(\mu U/\gamma)^{2/9} + 2.24(\mu U/\gamma)^{1/3}.$$

However this is not very useful because most of the physically interesting cases are where the capillary number exceeds the limit used in this analysis. This means surface tension would not dominate and the approaches used here would be useless.

Some interesting extensions of this work would be to explore the role surfactants play in the behavior of the bubble, and to explore the regimes outside of the limited arenas explored in this paper. However, the approach would have to be greatly modified as many of the critical assumptions would then become invalid.

References

- Brashforth, F. & Adams, J. C. 1883 *An Attempt to Test the Theories of Capillary Action*. Cambridge University Press.
- Bretherton, F. P. 1961 *J. Fluid Mech.* **10:2**, 166.
- Fairbrother, F. & Stubbs, A. E. 1935 *J. Chem. Soc.* **1**, 527.
- Fordham, S. 1948 *Proc. Roy. Soc. A* **194**, 1.
- Landau, L. & Levich, B. 1942 *Acta Physicochimica U.R.S.S.* **17**, 42.
- Marchessault, R. N. & Mason, S. G. 1960 *Ind. Engng. Chem.* **52**, 79.
- Panton, R. L. 1933 *Incompressible Flow*. 2nd ed. Wiley-Interscience.
- Probstein, R. F. 1994 *Physicochemical Hydrodynamics*. Wiley-Interscience.
- Prothero, J. W. & Burton A. C. 1962 *Biophysical Journal*. **2**, 199.
- Slavik, B. Z. & Jarvis, M. S. 1974 *Methods of Studying Plant Water Relations*. Taylor & Francis.
- Taylor, G. I. 1961 *J. Fluid Mech.* **10:1**, 161.